Available online at www.sciencedirect.com
SCIENCE DIRECT®
International Journal of Heat and Mass Transfer 48 (2005) 5081–5088
International Journal of HEAT and MASS TRANSFER
www.elsevier.com/locate/ijhmt

Technical Note

Dual influence of temperature and gas composition of selected helium-based binary gas mixtures on the thermal convection enhancement in Rayleigh–Bénard enclosures

Mohammad M. Papari [a], Darren L. Hitt [b], Antonio Campo [b,*]

[a] Department of Chemistry, College of Sciences, Shiraz University, Shiraz 71454, Iran
[b] Department of Mechanical Engineering, The University of Vermont, Burlington VT 05405, USA

Received 13 November 2003; received in revised form 14 June 2005
Available online 25 August 2005

Abstract

This paper addresses the potential augmentation of natural convection heat transfer in Rayleigh–Bénard enclosures when filled with a certain type of binary gas mixture. To form the binary gas mixtures, helium (He) is the primary gas and the secondary gases are nitrogen (N_2), oxygen (O_2), carbon dioxide (CO_2) and methane (CH_4). Each of the thermophysical properties participating in the binary gas mixtures viscosity η_m, thermal conductivity λ_m, density ρ_m, and heat capacity at constant pressure $C_{p,m}$ depends on the molar gas composition, temperature and pressure. Results are presented in terms of the maximum allied heat transfer coefficient $h_{m,max}/B$ at the optimal mole gas composition w_{opt}, in the w-domain $[0, 1]$ for the entire range of laminar and turbulent conditions. In the conduction regime, He provides the best heat transfer regardless of temperature. In the convection regime at 300 K a He–CO_2 mixture usually provides the maximum heat transfer, whereas at 1000 K pure methane CH_4 is the optimum. In addition, a detailed thermo-fluidic structure of the thermal convection patterns in the Rayleigh–Bénard enclosure was analyzed by performing 2-D numerical simulations.

Keywords: Rayleigh–Bénard enclosures; Binary gas mixtures; Heat transfer intensification; Optimal molar gas composition

1. Introduction

It is widely known that natural convection is regarded as an attractive mode of cooling when simplicity, economy, reliability and noise become constraint parameters of importance in engineering design. In view of these favorable attributes, natural convection has been the subject of considerable interest in the cooling of a variety of industrial devices, e.g., electric transformers, HVAC equipment, electronic packages, etc. An important subclass of problems on natural convection deals with confined flows inside stationary enclosures when a temperature differential is prescribed at two opposing walls. State-of-the-art review articles on natural convection inside stationary enclosures have appeared in the literature regularly (Hoogendoorn [1] and Yang [2]).

As pointed out by Bergles [3], when natural convection occurs, the enhancement of heat transport becomes

* Corresponding author. Tel.: +1 802 656 0978; fax: +1 802 656 1929.
E-mail address: acampo@cem.uvm.edu (A. Campo).

0017-9310/$ - see front matter © 2005 Elsevier Ltd. All rights reserved.
doi:10.1016/j.ijheatmasstransfer.2005.06.010

Nomenclature

A	heat exchange area (m^2)
B	overall coefficient related to h_m
C_p	heat capacity at constant pressure ($J\,m^{-3}\,K^{-1}$)
d	wall spacing (m)
g	acceleration of gravity ($m\,s^{-2}$)
h	heat transfer coefficient ($W\,m^{-2}\,K^{-1}$)
h_a	heat transfer coefficient of air ($W\,m^{-2}\,K^{-1}$)
h_m	heat transfer coefficient of a binary gas mixture ($W\,m^{-2}\,K^{-1}$)
m	molecular mass (kg)
M_i	molar mass of gas i ($kg\,mol^{-1}$)
M_m	molar mass of a binary gas mixture ($kg\,mol^{-1}$)
Nu	Nusselt number, hd/λ
Q	heat transfer rate (W)
Ra	Rayleigh number, $g\beta(\rho C_p/\eta\lambda)(T_h - T_c)d^3$
T_c	cold wall temperature (K)
T_m	mean temperature, $(T_h + T_c)/2$, (K)
T_h	hot wall temperature (K)
x_i	mole fraction of gas i
w	molar gas composition
w_{opt}	optimal molar gas composition

Greek symbols

β	coefficient of thermal expansion (K^{-1})
η	viscosity (μPa s)
λ	thermal conductivity ($W\,m^{-1}\,K^{-1}$)
ρ	density ($kg\,m^{-3}$)

Subscripts

m	mixture of binary gases
max	maximum

a difficult task because of the low fluid velocities that are generated by the gravitational flows. Owing to this adverse effect, it is of interest to explore power-independent instruments that are capable of augmenting the heat transfer without modifying the walls in contact with the fluid. Thereby, the present paper is centered in the study of the Rayleigh–Bénard enclosure with the objective of investigating the heat transfer capabilities of various binary gas mixtures formed with helium that are unattainable by: (a) each pure gas or (b) air.

It is expected that the outcome of the current study on RB enclosures will serve as a "proof-of-concept" in order to warrant maximum levels of heat transport by either internal or external natural convection without resorting to active or passive features that are more expensive. The results of this paper may be useful for both fundamental and applied research scenarios.

2. Heat transport in a Rayleigh–Bénard enclosure

A Rayleigh–Bénard enclosure (hereafter the RB enclosure) is defined as an enclosed space long and wide in the horizontal direction. The enclosed space is bounded by two large horizontal walls held at uniform temperatures, the lower wall at a temperature T_h higher than the upper wall at a temperature T_c (Gebhart et al. [4]). The coolant is normally a single-phase Newtonian liquid or a single gas.

The physics of fluids stipulates that the natural convection heat transport in a RB enclosure happens by two modes [4]. The first mode is prototypical of molecular conduction of heat in the layer of quiescent fluid that separates the two horizontal walls. In this mode, the buoyant forces are weak and cannot overcome the viscous forces creates an imbalance of forces. Consequently, the molecular conduction mode is governed by a linear temperature variation and the transfer of heat across the fluid layer is portrayed by a unitary Nusselt number $Nu = 1$. The plain pattern remains unaltered up to the attainment of a critical Rayleigh number $Ra_{crit} \approx 1708$ [4]. When the temperature differential $T_h - T_c$ is raised gradually, the buoyancy forces are intensified, and eventually outweigh the viscous forces. The fluid movement coupled with molecular heat conduction brings a second mode of heat transport [4]. This situation is connected to moderate-to-large values of Ra numbers inside the ample sub-interval $1708 < Ra < 3.2 \times 10^5$. Under these circumstances, the fluid possesses laminar motion and takes the form of 2-D regularly spaced counter-rotating roll cells of square cross-section. These cells are traditionally recognized as Bénard cells in honor of Bénard [5] who first reported this singular phenomenon back in 1900. Further increases in the temperature differential $T_h - T_c$ exceed the upper limit $Ra = 3.2 \times 10^5$, carrying 2-D roll cells that break apart and immediately form 3-D cells of hexagonal shape when viewed from above. At even higher $Ra \gg 3.2 \times 10^5$, the natural convective flow energizes further, the number of 3-D cells multiply, turn narrower and the flow becomes turbulent and oscillatory.

The rate of heat transport Q in a RB enclosure is calculated from "Newton's law of cooling"

$$Q = hA(T_h - T_c). \tag{1}$$

For the estimation of the heat transfer coefficient h in a RB enclosure, the first experimental-based correlation equation was constructed by Jakob [6]

$$Nu = CRa^n, \tag{2}$$

where the length scale in Nu and Ra is the wall spacing d. Eq. (2) covers all regular gases contained in the Prandtl number band $0.5 \leqslant Pr \leqslant 2$. In this equation, the thermo-physical properties of the gases are evaluated at a mean temperature $T_m = (T_h + T_c)/2$.

The accuracy of the correlation equations for RB enclosures has been profusely validated theoretically, numerically and experimentally over the subsequent years as reflected in the publications by Goldstein and Chu [7] and Hollands et al. [8].

3. Levels of heat transport imparted by binary gas mixtures

First, at sub-critical Rayleigh numbers $Ra < 1708$, the mode of molecular conduction of heat in a RB enclosure predominates; this mode relies on one transport property, the thermal conductivity λ. Clearly, in the reduced Ra sub-interval the sole way for enhancing the heat transport is to choose a gas owing a high thermal conductivity, say for instance helium (He). Second, for super-critical Rayleigh numbers $Ra > 1708$, the thermal buoyancy forces in the RB enclosure are stimulated and a circulatory gas motion is induced. The objective now is to invigorate the mode by natural convection of heat (comprising molecular conduction and gas motion) exploring certain binary gas mixtures as suitable gaseous media for heat transfer intensification. In this study, four binary gas mixtures have been selected where the primary component is helium (He) and the secondary components are nitrogen (N_2), oxygen (O_2), carbon dioxide (CO_2) and methane (CH_4).

Let h_m designate the heat transfer coefficient for a binary gas mixture. Thereby, from Eq. (2), h_m varies with four thermo-physical properties: viscosity η_m, thermal conductivity λ_m, density ρ_m and heat capacity at constant pressure $C_{p,m}$ establishing the function

$$h_m = B\left(\frac{\rho_m C_{p,m}}{\eta_m}\right)^n \lambda_m^{1-n}, \tag{3}$$

where the subscript m denotes mixture of binary gases. In this relation, the new coefficient B equates to $\{[Cg\beta(T_h - T_c)d^3]^n\}$. Since for an ideal gas $\beta = 1/T_f$, B is independent of the nature of the binary gas mixture. Therefore, the ratio h_m/B may be interpreted as an allied heat transfer coefficient representative of a binary gas mixture. When the fluid is a binary gas mixture, each of the thermo-physical properties η_m, λ_m, ρ_m, and $C_{p,m}$ varies with temperature T, pressure P and the molar gas composition w by way of individual functions $f(w,p,T)$.

The molar gas composition w_i of a binary gas mixture is defined as

$$w_i = \frac{x_i M_i}{M_m}, \quad i = 1,2, \tag{4}$$

where x_i is the mole fraction, M_i is the molar mass of component i, and $M_m = x_1M_1 + x_2M_2$ is the molar mass of the binary gas mixture ([9]).

4. Discussion of results

Engineering designs of gas-filled RB enclosures rest on three principal elements that act in unison: (1) the wall spacing δ, (2) the applied temperature difference $T_h - T_c$, and (3) the working gas. We set aside item (1) and focus our attention on items (2) and (3).

Owing that air is the most commonly used coolant in industry, it was deemed appropriate to compare the heat transfer performance of a RB enclosure filled with air against four identical RB enclosures filled with the binary gas mixtures: He–N_2, He–O_2, He–CO_2 and He–CH_4. The influence of the mean temperature $T_m = (T_h + T_c)/2$ and gas composition w was examined with two cases one at a low temperature $T_f = 300$ K and the other at a high temperature $T_f = 1000$ K both at atmospheric pressure $P = 1$ atm.

A typical figure displays the allied heat transfer coefficient h_m/B versus the molar gas composition w. In the abscissa the left extreme $w = 0$ corresponds to pure He, whereas the right extreme $w = 1$ corresponds to the other component N_2, O_2, CO_2 and CH_4. The figure also includes a horizontal line indicative of h_m/B for air, the baseline case.

4.1. Low mean temperature of 300 K

The exponent $n = 0$ applies to the sub-critical $Ra_{crit} < 1708$. This first sub-interval is attached to the mode of molecular conduction, which is characterized by a single thermo-physical property, the thermal conductivity λ. Among the five pure gases, it is clear that the largest allied heat transfer coefficient, $h_{m,max}/B$, is furnished by helium (He). For an exponent $n = 1/4$ corresponding to the third Ra sub-interval in Table 1: $7 \times 10^3 < Ra < 3.2 \times 10^5$ no maximum for h_m/B is reached. This common behavior is insensitive to the components forming the binary gas mixtures, and signifies that the largest heat transfer coefficient $h_{m,max}/B$ takes place when the RB enclosure is filled with He, so that the optimal concentration of the gas mixture occurs at $w_{opt} = 0$. When compared to air (the baseline case), the heat transfer enhancement $(h_{m,max} - h_a)/h_a$ delivered by pure He reaches a remarkable value of 103%.

Table 1
Values of the coefficient C and the exponent n arising in Eq. (2)

Ra sub-intervals	C	n
Frst sub-interval <1708	1	0
Second sub-interval (1708, 7×10^3)	0.059	2/5
Third sub-interval (7×10^3, 3.2×10^5)	0.212	1/4
Fourth sub-interval >3.2×10^5	0.061	1/3

The four curves related to the exponent 1/3, the fourth *Ra* sub-interval: $Ra > 3.2\times10^5$ in Table 1 are discussed now. Here, the binary gas mixture He–CH_4 does not yield a maximum for the allied heat transfer coefficient h_m/B, whereas the pair of He–O_2 and He–N_2 gas mixtures exhibits mild maxima for h_m/B that are practically imperceptible. Relative to air, the heat transfer enhancement given by pure He is around 47% and the heat transfer enhancement $(h_{m,max} - h_a)/h_a$ of the He–CO_2 gas mixture is of the order of 56% occurring at the optimal concentration of $w_{opt} = 0.70$.

The behavior of the second exponent $n = 2/5$, responsible for the sub-interval $1.7\times10^3 < Ra < 7\times10^3$ in Table 1 is connected to Fig. 1. It is observable that in this case, the group of h_m/B curves exhibits definitive maxima. Among the four curves, the maximum allied heat transfer coefficient $h_{m,max}/B$ is delivered by the He–CO_2 gas mixture at the optimal molar gas composition $w_{opt} = 0.88$; the heat transfer intensification $(h_{m,max} - h_a)/h_a$ is of the order of 36%. With respect to air, the heat transfer intensification $(h_{m,max} - h_a)/h_a$ supplied by He experiences a meager 10% increment. The three other curves are pushed down in the following order: first He–CH_4, second He–O_2, and third He–N_2. The respective optimal molar gas compositions w_{opt} are shifted to the left of $w_{opt} = 0.88$.

4.2. High mean temperature of 1000 K

Attention is directed to the variation of the allied heat transfer coefficient h_m/B with the molar gas concentration w for the four binary gas mixtures regulated by an exponent $n = 1/4$ in the third *Ra* sub-interval: $7\times10^3 < Ra < 3.2\times10^5$ in Table 1. The curves for the three binary gas mixtures He–CO_2, He–N_2 and He–O_2 turn down, as w increases revealing no heat transfer maxima. In contrast, the curve for the remaining He–CH_4 gas mixture turns up as w grows exhibiting a monotonic behavior that reaches its peak at $w = 100\%$. This particular trend reflects that the pure gas methane (CH_4) and not the He–CH_4 gas mixture, produces the maximum heat transfer coefficient. Qualitatively, the one-to-one comparison between CH_4 and air (the baseline case) results in a vigorous heat transfer enhancement $(h_{m,max} - h_a)/h_a$ for the former gas of the order of 140%.

When the exponent n moves up to $n = 1/3$ linked to the fourth *Ra* sub-interval: $Ra > 3.2\times10^5$ in Table 1, insignificant maxima for the allied heat transfer coefficient h_m/B are observed for the two binary gas mixtures He–N_2 and He–O_2. Although the curve for the He–O_2 gas mixture lies above the curves for the He–N_2 and He–O_2 gas mixtures, the trend evidences a moderate

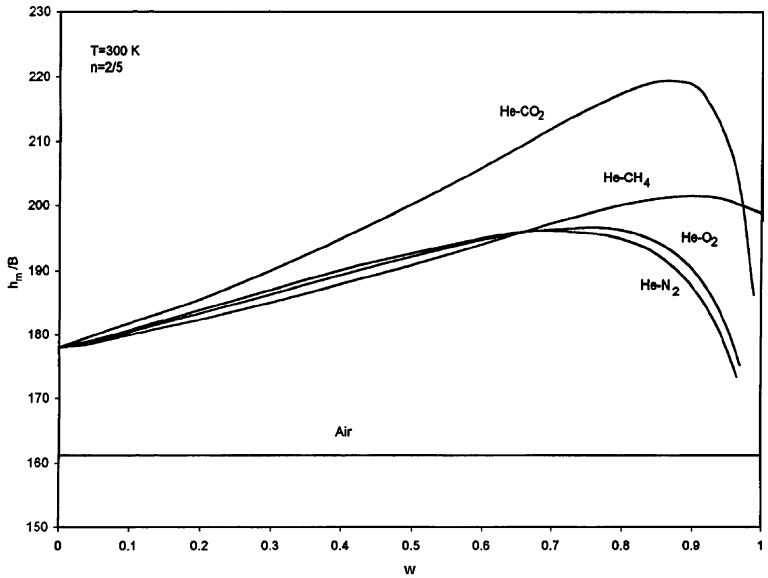

Fig. 1. Variation of the allied heat transfer coefficient h_m/B with the molar gas concentration w of the binary gas mixtures for $n = 2/5$ at 300 K.

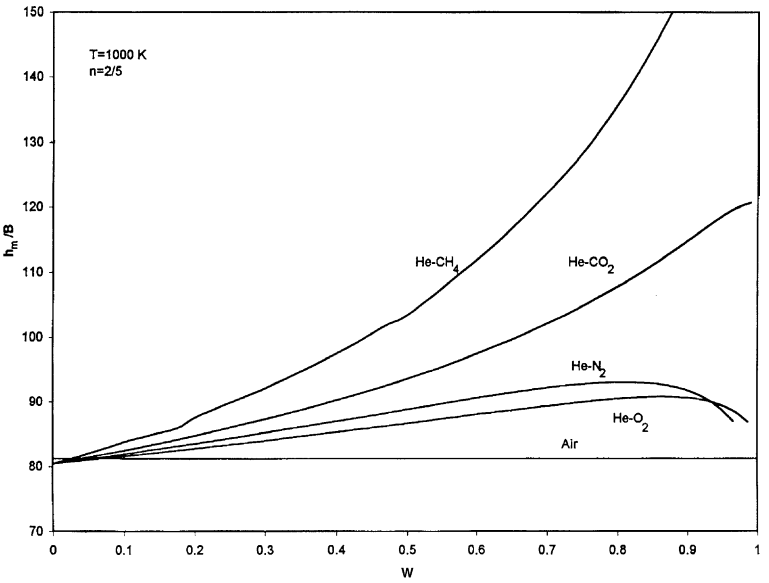

Fig. 2. Variation of the allied heat transfer coefficient h_m/B with the molar gas concentration w of the binary gas mixtures for $n = 2/5$ at 1000 K.

maximum for h_m/B. The salient aspects of this figure are the ascending monotonic pattern displayed by the He–CH_4 gas mixture, and the magnitude of the allied heat transfer coefficient h_m/B gets intensified as w increases. Here again, the global maximum for the allied heat transfer coefficient $h_{m,max}/B$ is reached at $w = 100\%$, this value is connected to pure methane gas (CH_4). As compared to air, a significant heat transfer enhancement $(h_{m,max} - h_a)/h_a$ of 138% is supplied by CH_4.

Results for the largest exponent $n = 2/5$ corresponding to the second sub-interval $1708 < Ra < 7 \times 10^3$ in Table 1 are plotted in Fig. 2. Literally, the family of curves follows a pattern similar to its counterpart for the exponent $n = 1/3$. Pure gas methane (CH_4) is responsible for the maximum heat transfer coefficient $h_{n,max}/B$, bringing along with it a heat transfer enhancement $(h_{m,max} - h_a)/h_a$ of order 132% as compared to air, the baseline case.

5. Numerical simulations

In the preceding sections of this paper, the focus has been on the prediction and maximization of convective heat transfer characteristics of different binary gas mixtures based upon a thermodynamic analysis of the mixture properties. Here we shall examine the detailed thermo-fluidic structure of the convection patterns by performing 2-D numerical simulations of the Rayleigh–Bénard enclosure. The goal is to gain additional dynamical insight and obtain possible explanation(s) for the existence of optimal mixture concentrations, thereby bridging with our knowledge obtained from the thermodynamic analyses.

5.1. Computational method

A schematic diagram of the geometry of the Rayleigh–Bénard enclosure for the case study appears in Fig. 3. The domain is bounded above and below by cold and hot rigid plates, respectively, of width $2w$ and separated by a uniform gap h. The right boundary is taken to be an insulated rigid wall and the left boundary is a symmetry plane. In the limit of $w/h \gg 1$ the idealized case of 2-D Bénard convection between the infinite parallel plates is recovered. In the present study we assume a gap width of $h = 10$ cm and a plate half-width of

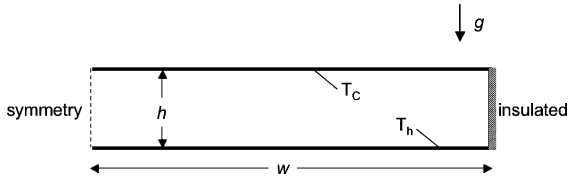

Fig. 3. Schematic drawing of the geometry and boundary conditions used in the 2-D computational model. The upper and lower boundaries consist of rigid isothermal plates at temperatures T_c and T_h, respectively. The right boundary is a rigid insulated wall and the left boundary is a symmetry plane. The full domain has an aspect ratio of $2\,w/h$, which is taken to be sufficiently large as to well approximate the Rayleigh–Bénard problem for two infinite plates. In the numerical simulations $w = 1$ m, $h = 0.1$ m and the temperature differential ΔT is 20 K.

$w = 1$ m which provides an aspect ratio of 20-to-1. Given the specified geometry and temperature differential $T_h - T_c$, along with the thermo-physical properties of the gas mixture, the Rayleigh number for the flow is adjusted by setting the value of the gravitational constant g.

A computational mesh has been constructed using the GAMBIT2.0® grid generator software (Fluent Inc.). Owing to the simplicity of the domain the mesh consists completely of quadrilateral elements with zero-skewness. A uniform grid resolution of 0.25 cm has been chosen for the horizontal and vertical directions; for the dimensions given above, this results in a modest mesh size of 16,000 elements. More refined grids having uniform resolutions of 0.10 cm and 100,000 elements have also been considered; however the computed heat flux between the two grid resolutions have been found to differ by less than 0.25%. The coarser (0.25 cm) resolution has thus been deemed quite adequate for the purposes of this study given the significant reduction in computational effort.

The steady-state flow is governed by the 2-D coupled equations of mass, momentum, and energy conservation, along with the equation of state; here we assume the gas mixture behaves as a perfect gas. The governing equations are solved using the FLUENT6® computational fluid dynamics software package, which is based on the finite volume method. In all numerical studies performed, a constant temperature differential ($T_h - T_c$) of 20 K has been imposed between the plates. Given the small temperature differential between the upper and lower plates, all thermo-physical properties of the gas mixture (except density) are taken as constants and evaluated at the mean temperature $(T_h + T_c)/2$. An implicit segregated solver was used and all discretization schemes employed are of second-order accuracy or higher. The QUICK scheme was used for the momentum, energy and density discretization. A second-order body-force-weighted scheme was used in the pressure discretization and the SIMPLE scheme was used in the pressure–velocity coupling. Convergence of a simulation was assessed through the monitoring of computed residuals (velocity, energy and mass conservation) and also through the convergence of point and/or surface monitors for velocity, temperature and heat flux at selected locations in the domain.

Once a solution was obtained, the local heat flux distribution was computed on the lower (or upper) plate and then integrated over the entire surface to obtain the total heat transfer rate. Referring to Fig. 3, the Nusselt number for the simulation was determined by

$$Nu = \frac{Qh}{\lambda w(T_h - T_c)}, \tag{5}$$

where Q is the total heat transfer rate per unit depth.

5.2. Numerical results for low and high temperatures

Numerical simulations for different gas mixtures were performed under parametric conditions corresponding to the first Rayleigh subinterval ($Ra_{crit} < Ra < 7000$, $n = 2/5$). Scenarios having mean operating temperatures of 300 K and 1000 K, respectively, have been considered. These selections were made on the basis that the preceding thermodynamics analyses of Section 4 predict the existence of an optimum mixture ratio at 300 K and the absence of an optimum mixture at 1000 K for this Rayleigh subinterval. Given the domain geometry (Fig. 3) and the thermo-physical properties of He–CH_4 mixtures, a value of the gravitational constant was chosen so as to ensure that a span of mixture ratios yielded Rayleigh numbers which fell within the first subinterval. For the case of the 300 K operating temperature, a substantially reduced value of $g = 0.055$ m/s^2 was chosen whereas a value of $g = 5.0$ m/s^2 was chosen for the 1000 K case. With these respective choices for gravity, cases with mixture ratios ranging from 50% to 100% CH_4 fell within the first Rayleigh subinterval.

Shown in Fig. 4 are the results for a 50% CH_4 gas mixture at a mean operating temperature of 300 K.

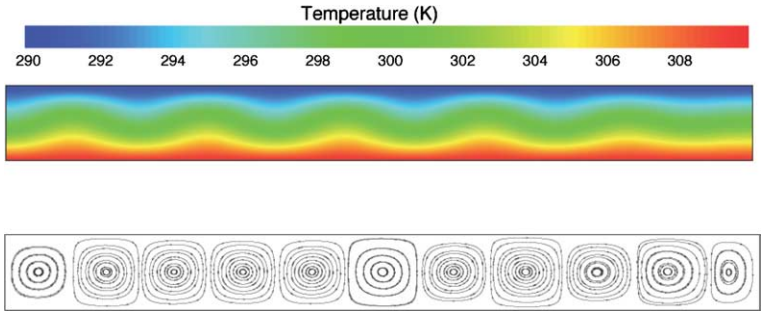

Fig. 4. Numerical results for a 50% He–CH_4 mixture of and a mean temperature of 300 K. Shown is a contour plot of the temperature field (top) along with a plot of the streamlines (bottom). The gravitational constant was set to 0.055 m/s^2, which yields a Rayleigh number of 1807. For these conditions the natural convection is very weak; the maximum stream function is $\psi_{max} = 3.76 \times 10^{-5}$ kg/s.

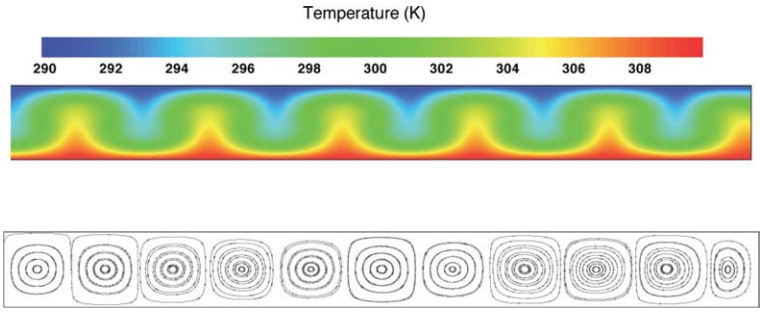

Fig. 5. Numerical results for an "optimal" mixture of 75% CH_4 and a mean temperature of 300 K. Shown is a contour plot of the temperature field (top) along with a plot of the streamlines (bottom). The gravitational constant was set to 0.055 m/s^2, which yields a Rayleigh number of 4222. For these conditions the natural convection is considerably stronger than the 50% mixture. The maximum stream function is $\psi_{max} = 1.79 \times 10^{-4}$ kg/s which implies a circulation roughly an order of magnitude greater.

For the parametric conditions previously indicated, this mixture proved just sufficient to generate a very weak natural convection flow ($Nu \sim 1.05$); for lower concentrations of CH_4 the heat transfer remained purely conductive. At seen in the temperature contour plot, only a minor sinusoidal perturbation to the stratified conduction profile is produced. The corresponding roll pattern in the flow has a characteristic cell size of 0.18 m or approximately 9% of the enclosure width. In contrast, when the mixture concentration is increased to 75% CH_4 a much stronger convection pattern is observed (Fig. 5). The temperature field features an alternating array of localized maxima and minima, which extend from the lower and upper plates, respectively, and penetrate well into the core region of the flow. The size of the convection cells remains unchanged although the circulation increases significantly as evidenced by the maximum stream function values ($\psi_{max,50\%} = 3.76 \times 10^{-5}$ kg/s; $\psi_{max,75\%} = 1.79 \times 10^{-4}$ kg/s). For CH_4 concentrations above 75% it is found the circulation continues to increase but at reduced and nearly linear rate. Further, there is no appreciable change in the flow pattern or structure of the temperature field.

The heat transfer results for different gas mixtures at 300 K are summarized in Fig. 6. Here an interesting feature is observed. The Nusselt number for the RB enclosure increases monotonically as the gas mixture tends towards 100% CH_4. On the other hand, a local maximum in the heat transfer coefficient h (or, equivalently, the heat transfer rate) is found at a mass fraction of approximately 75% CH_4. At mass fractions above this "optimal value" there is a modest downward trend in the heat transfer coefficient. We note that the optimal mixture mass fraction of 75% is slightly higher than the theoretical prediction of ~70% (mole fraction of $w \sim 0.9$, see Fig. 1). We suspect the minor discrepancy in the optimal concentrations can be attributed to differences inherent in the approaches used. The theoretical prediction was derived for idealized 2-D Rayleigh–Bénard flow between infinite plates whereas the present

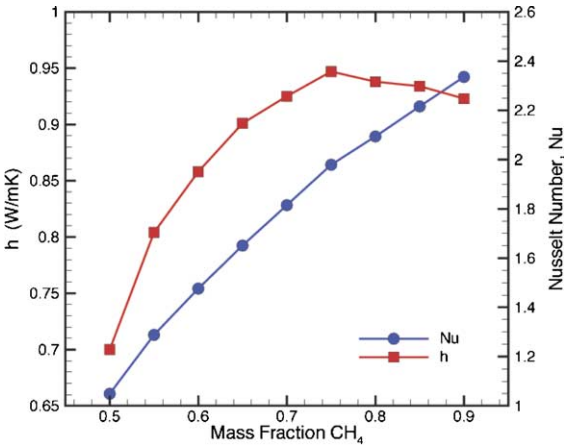

Fig. 6. Results showing the heat transfer coefficient (squares) and the Nusselt number (circles) as a function of the CH_4 concentration for a mean temperature of 300 K. The maximum heat transfer occurs at a mixture of approximately 75% CH_4. In contrast, the Nusselt number increases monotonically over this range and lacks any local maximum.

CFD model can only approximate such conditions on a finite geometry. Further, the presence of the rigid side walls clearly reduces the flow circulation as evidenced in the right-most convection cells in Figs. 4 and 5. These differences aside, there is nothing striking in the computed velocity and temperature fields that is indicative of an optimal mass fraction in the mixture range of 70–75% CH_4. The lack of an overt fluid-mechanical explanation for the optimization instead suggests that the enhancement of heat transfer is due to the subtle interplay of the thermo-physical properties of the binary gas mixture.

When the mean temperature of the gas mixtures is increased to 1000 K, a different heat transfer behavior is found. At this higher temperature, it is found that the threshold mass fraction for the onset of natural convection increases to ~75% CH_4. For mass fractions between

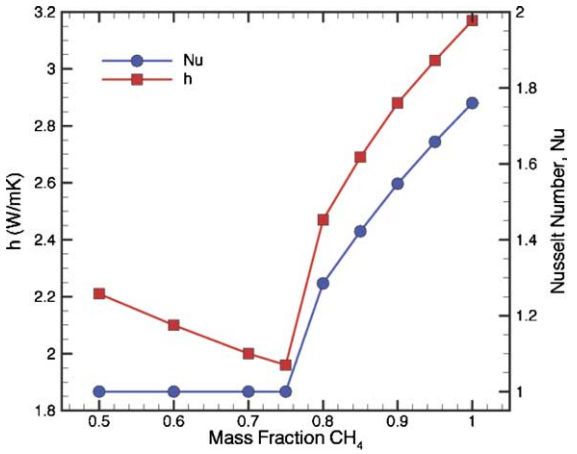

Fig. 7. Results showing the heat transfer coefficient (squares) and the Nusselt number (circles) as a function of the CH_4 concentration for a mean temperature of 1000 K. At this elevated temperature a threshold concentration of approximately 75% CH_4 is required for the onset of natural convection. Below this value the heat transfer is remains purely conductive ($Nu = 1$). It is interesting to note that the critical mixture represents a local minimum for the total heat transfer. At lower mixture concentrations the heat transfer increases due to a reduced thermal conductivity of the mixture whereas natural convection promotes greater heat transfer at higher concentrations.

50% and 75% CH_4 a state of pure conduction exists ($Nu = 1$); however the heat transfer coefficient, and hence the heat transfer rate, decreases in a nearly linear manner towards a local minimum at 75% CH_4. This trend is obviously due to the mixture-dependent decrease in the thermal conductivity of the gas over this range. At mass fractions above 75% CH_4 the onset and subsequent strengthening of the natural convection results in a monotonic increase in the heat transfer coefficient (and Nusselt number) which is maximized at 100% CH_4. It is interesting to observe that for heat transfer coefficients between 1.96 W/m K and 2.2 W/m K there are actually two possible mixture concentrations that yield that value; the lower concentration accomplishes this through pure conduction whereas the higher concentration does so through convection. Extrapolation of the numerical data to lower concentrations not simulated suggests this multi-valued character of the heat transfer can be extended over a broader range of concentrations than directly observed in Fig. 7.

6. Conclusions

Based on the four He-based binary gas mixtures He–N_2, He–O_2, He–CO_2 and He–CH_4 to be employed in Rayleigh–Bénard enclosures, the main conclusions that can be drawn for heat transfer intensification are summarized now. For atmospheric pressure and a low temperature of 300 K, there is no discernible maximum for the allied heat transfer coefficient, h_m/B among the four binary gas mixtures. Thereby, pure helium (He) is the best alternative for *Ra* sub-intervals linked to the smallest exponent $n = 1/4$ in Table 1. The He–CO_2 gas mixture is unequivocally the best candidate gas for the *Ra* sub-intervals connected to the two exponents $n = 1/3$ and 2/5. Meanwhile, for the same pressure and a high temperature of 1000 K, pure methane (CH_4) is the best gas choice for RB enclosures that fall into the *Ra* sub-intervals governed by the exponents $n = 1/4$, 1/3 and 2/5.

References

[1] C.J. Hoogendoorn, Natural convection in enclosures, Proceedings of 8th International Heat Transfer Conference, 1, 1986, p. 111.
[2] K.T. Yang, Natural convection in enclosures, in: S. Kakac et al. (Eds.), Handbook of Single-Phase Heat Transfer, John Wiley, New York, 1987 (Chapter 13).
[3] A.E. Bergles, Techniques to Augment Heat Transfer, in: W.M. Rosehnow et al. (Eds.), Handbook of Heat Transfer, third ed., McGraw-Hill, New York, 1999 (Chapter 11).
[4] B. Gebhart, Y. Jaluria, R.L. Mahajan, B. Sammakia, Buoyancy-induced flows and transport, Hemisphere, New York, 1988.
[5] H. Bénard, Les tourbillons cellulaires dans une nappe liquide transportant de la chaleur par convection en régime permanent, Ann. Chim. Phys. 23 (1900) 62–144.
[6] M. Jakob, Free convection through enclosed gas layers, Trans. ASME 68 (1946) 189–195.
[7] R.J. Goldstein, T.Y. Chu, Thermal convection in a horizontal layer of air, Prog. Heat Mass Transfer 2 (1969) 55–59.
[8] K.G.T. Hollands, Free convective heat transfer across inclined air layers, ASME J. Heat Transfer 98 (1976) 189–193.
[9] B.E. Polling, J.M. Prausnitz, J.P. O'Connell, The Properties of Gases and Liquids, McGraw-Hill, New York, 2001, pp. A5–A19.